Long-Acting Neurotensin Synergizes With Liraglutide to Reverse Obesity Through a Melanocortin-Dependent Pathway

Cecilia Ratner,[1,2] Zhenyan He,[3] Kaare V. Grunddal,[2] Louise J. Skov,[1,2] Bolette Hartmann,[1,2] Fa Zhang,[4] Annette Feuchtinger,[5] Anette Bjerregaard,[1,2] Christina Christoffersen,[2,6] Matthias H. Tschöp,[7,8] Brian Finan,[9] Richard D. DiMarchi,[4] Gina M. Leinninger,[10] Kevin W. Williams,[3] Christoffer Clemmensen,[1] and Birgitte Holst[1,2]

Neurotensin (NT), a gut hormone and neuropeptide, increases in circulation after bariatric surgery in rodents and humans and inhibits food intake in mice. However, its potential to treat obesity and the subsequent metabolic dysfunctions have been difficult to assess owing to its short half-life in vivo. Here, we demonstrate that a long-acting, pegylated analog of the NT peptide (P-NT) reduces food intake, body weight, and adiposity in diet-induced obese mice when administered once daily for 6 days. Strikingly, when P-NT was combined with the glucagon-like peptide 1 mimetic liraglutide, the two peptides synergized to reduce food intake and body weight relative to each monotherapy, without inducing a taste aversion. Further, P-NT and liraglutide coadministration improved glycemia and reduced steatohepatitis. Finally, we show that the melanocortin pathway is central for P-NT–induced anorexia and necessary for the full synergistic effect of P-NT and liraglutide combination therapy. Overall, our data suggest that P-NT and liraglutide combination therapy could be an enhanced treatment for obesity with improved tolerability compared with liraglutide monotherapy.

The prevalence of obesity and diabetes has reached epidemic proportions and is still on the rise (1). Despite this, a limited number of antiobesity drugs are currently approved, including the glucagon-like peptide 1 (GLP-1) analog liraglutide. However, liraglutide and other obesity pharmacotherapies evoke only modest weight loss of 5–10% (2). For improvement of efficacy and limiting of unacceptable adverse effects, a current innovation in the development of antiobesity treatments involves targeting multiple signaling pathways simultaneously. This approach has several advantages including exploiting additive or synergistic effects between distinct signaling pathways and is supported by the marked weight loss associated with bariatric surgery, which broadly stimulates anorexigenic hormone release (3). Further, tolerability is expected to improve with combination treatments, as lower doses of each agent could be used. With monotherapy, adverse effects are often reported due to the usage of peak doses. For example, upward of 30–40% of patients on therapeutic doses of liraglutide suffer from nausea in a dose-dependent manner (4,5).

Combinatorial treatment approaches have thus far largely been explored for GLP-1 mimetics (6) in combination with a range of other hormones including leptin (7), peptide YY (PYY) (8), cholecystokinin (9), amylin (10), and

[1]Novo Nordisk Foundation Center for Basic Metabolic Research, University of Copenhagen, Copenhagen, Denmark
[2]Department of Biomedical Sciences, University of Copenhagen, Copenhagen, Denmark
[3]Division of Hypothalamic Research, Department of Internal Medicine, University of Texas Southwestern Medical Center at Dallas, Dallas, TX
[4]Department of Chemistry, Indiana University, Bloomington, IN
[5]Research Unit Analytical Pathology, Helmholtz Zentrum München, Munich, Germany
[6]Department of Clinical Biochemistry, Rigshospitalet, Copenhagen, Denmark
[7]Institute for Diabetes and Obesity, Helmholtz Diabetes Center, Helmholtz Zentrum München, Munich, Germany
[8]Division of Metabolic Diseases, Department of Medicine, Technische Universität München, Munich, Germany
[9]Novo Nordisk Research Center Indianapolis, Indianapolis, IN
[10]Department of Physiology, Michigan State University, East Lansing, MI

Corresponding author: Cecilia Ratner, cecilia.ratner@sund.ku.dk

Received 18 September 2018 and accepted 18 March 2019

glucagon/glucose-dependent insulinotropic polypeptide (11) either as adjunctive cotreatments or as coagonist fusion peptides. We recently demonstrated that, in addition to the expression in N-cells, the gut hormone neurotensin (NT) is coexpressed with GLP-1 and PYY in L cells (12), suggesting a common functional importance.

NT is generally considered an anorexigenic neuropeptide and reduces food intake when administered directly into the brain (13–15). Further, NT is increased in circulation following gastric bypass surgery in rodents and humans (16–18), which we demonstrated might contribute to the subsequent hypophagia (16). The metabolic effects of peripheral NT are, however, incompletely understood, which may relate to the challenges working with peptide hormones with short circulatory half-lives such as NT, where the half-life is estimated to 30 s in rodents (19). To improve the understanding of NT effects on metabolism, we have developed a long-acting NT peptide (pegylated NT [P-NT]) (16). P-NT prolongs the inhibition of feeding in mice at least 10 times compared with native NT (16), but its effects in a chronic setting as well as its downstream targets are incompletely understood. We hypothesized that long-acting NT and GLP-1 mimetics converge in the central melanocortin pathway but through different intracellular signaling pathways, $G\alpha_q$ and $G\alpha_s$, respectively, to reduce food intake and reverse obesity.

RESEARCH DESIGN AND METHODS

Animals
Male C57Bl/6J mice (Janvier, Le Genest-Saint-Isle, France) were used as wild-type lean or diet-induced obese (DIO) mice. DIO mice were fed a high-fat, high-sucrose diet (58% fat, cat. no. D12331; Research Diets, New Brunswick, NJ) from 7 weeks of age for 4–6 months. Lean mice were fed a chow diet (1310; Altromin, Lage, Germany). Mice were housed in temperature-controlled environments under a 12/12 h light-dark cycle with ad libitum access to food and water unless otherwise stated. Animal experiments using wild-type lean or DIO mice and male loxTB melanocortin 4 receptor (MC4R) mice (20) (B6;129S4-$Mc4r^{tm1Lowl}$/J, stock no. 006414; The Jackson Laboratory, Bar Harbor, ME) were approved by the Danish animal inspectorate or the Animal Use and Care Committee of Bavaria, Germany, and followed institutional guidelines. Electrophysiology studies using Pomc-hrGFP mice (21) were performed in accordance with the guidelines established by the National Institutes of Health Guide for the Care and Use of Laboratory Animals and approved by the University of Texas Institutional Animal Care and Use Committee.

Peptides
The side-chain protected NT with a KKGG linker at N-terminal was assembled by automated synthesis using an ABI-433A peptide synthesizer with standard Fmoc/6-Cl-HOBt/DIC coupling protocols. The crude peptide was acylated with 20 kDa α-methoxy-ω-carboxylic acid succinimidyl ester poly(ethylene glycol) (MeO-PEG-NHS) (Iris Biotech GmbH, Marktredwitz, Germany). The desired PEG-peptide was purified by preparative reverse-phase high-performance liquid chromatography, final peptide deprotection was conducted, and a second preparative high-performance liquid chromatography purification was performed. Matrix-assisted laser desorption/ionization analysis confirmed the molecular weight of the final product.

Liraglutide was provided by Novo Nordisk (Indianapolis, IN, or Måløv, Denmark). All peptides were solubilized in saline. Liraglutide was dosed in a concentration of 2, 3, or 8 nmol/kg equivalent of 7.5, 11.3, and 30 μg/kg, respectively, as indicated in figure legends. Importantly, to allow a sufficient window for weight loss synergy, subthreshold doses of liraglutide were used and each batch of liraglutide was independently dose optimized. P-NT was dose optimized in concentrations ranging from 44 to 1,188 nmol/kg in threefold increments in DIO mice both as a monotreatment and in combination with liraglutide. A dose of 396 nmol/kg P-NT was used in additional experiments. P-NT and liraglutide cotreatment was administered by single formulated injections. Peptides were dosed at a volume of 5 mL/kg subcutaneously.

Food Intake, Body Weight, and Indirect Calorimetry
DIO and MC4R knockout (KO) mice ($n = 5$–8 as indicated in figure legends) were single housed or housed in pairs and treated daily for 2–6 days as indicated in figures with vehicle, liraglutide, P-NT, or cotreatment with liraglutide and P-NT in the end of the light phase. One cohort of DIO mice ($n = 8$) was placed in an indirect calorimetry system (TSE Systems, Bad Homburg, Germany) during peptide treatment where food intake, respiratory exchange ratio (RER), energy expenditure, and activity levels were continuously monitored for 72 h. Body composition was assessed using MRI (EchoMRI, Houston, TX). MC4R KO mice were fed a high-fat, high-sucrose diet (D12331; Research Diets) for 5 weeks prior to pharmacological treatment. Weight-matched DIO C57Bl/6J mice served as controls for MC4R KO mice. After a 1-week washout period, the effect of a 10× dose of liraglutide (20 nmol/kg [75 μg/kg]) was assessed in MC4R KO and weight-matched DIO controls.

Tissue Collection for Blood Biochemistry, Liver Histology, and Quantitative PCR
Tissue was collected after 6 days of treatment in DIO mice. On the day of sacrifice, mice were fasted for 4 h, blood sampling was done from the tail vein and glucose was measured using a glucometer before mice received an injection of peptides before sacrifice and tissue collection 2 h later. Liver samples were immersed in 4% paraformaldehyde or snap frozen in liquid nitrogen, and plasma was collected in EDTA-coated tubes, centrifuged at 3,000g for 15 min at 4°C, and stored at −80°C.

Blood Biochemistry
Lipoprotein separation was performed using size exclusion chromatography with 120 μL pooled plasma from the

treatment groups as previously described (22). The following kits were used for remaining analyses: cholesterol (Thermo Scientific, Waltham, MA), triglycerides (Wako Chemicals, Neuss, Germany), insulin (Meso Scale Discovery, Rockville, MD), and leptin (Meso Scale Discovery).

Liver Histology

Excised liver samples were fixed in 4% formalin, embedded in paraffin, and cut into 3-μm slices for hematoxylin-eosin (H-E) staining. The H-E slides were evaluated using a brightfield microscope (Axioplan; Zeiss, Oberkochen, Germany). The steatohepatitis score was defined as the unweighted sum of the individual score for steatosis and lobular inflammation. Steatosis and lobular inflammation were scored as previously described (23). Total scores ranged from 0 to 6, with score 0 considered no steatohepatitis, scores 1 and 2 considered borderline steatohepatitis, scores 3 and 4 considered onset steatohepatitis, and scores 5 and 6 considered definite steatohepatitis.

Quantitative PCR

Liver RNA was extracted using the RNeasy Lipid Tissue Mini Kit (Qiagen, Hilden, Germany) with DNAse digestion according to the manufacturer's instructions. cDNA was synthesized from RNA-matched samples using the SuperScript III Reverse Transcriptase kit (Thermo Fisher Scientific). Quantitative PCR was performed using PrecisionPLUS Master Mix on a LightCycler 480 (Roche Applied Science, Penzberg, Germany). Relative gene expression was calculated using the $\Delta\Delta C_t$ method normalizing to the average value of the reference genes TATA-box binding protein (*TBP*) and hypoxanthine-guanine phosphoribosyltransferase (*HPRT*). See Supplementary Table 1 for primers.

Taste Aversion

Taste aversion was performed in lean mice (*n* = 8) as previously described (16). During conditioning, mice received injections of vehicle, liraglutide (3 nmol/kg), P-NT (396 nmol/kg), combination treatment with liraglutide (3 nmol/kg) and P-NT (396 nmol/kg), or LiCl (3 mmol/kg), which served as a positive control.

Pharmacokinetic Profiling

Lean mice (*n* = 4) were treated with vehicle, P-NT (396 nmol/kg), liraglutide (3 nmol/kg), or cotreatment with liraglutide (3 nmol/kg) and P-NT (396 nmol/kg). Blood was drawn from the tail vein at the indicated time points into EDTA-coated tubes, centrifuged at 3,000*g* for 15 min at 4°C, and stored at −80°C. Intact NT was measured as previously described (24).

Oral Glucose Tolerance Test

DIO mice (*n* = 14) were treated with a single dose of vehicle, liraglutide (2 nmol/kg), P-NT (396 nmol/kg), or combination treatment 1 h prior to glucose administration (1 g/kg p.o.) to assess the acute effect of the peptides on glucose tolerance. Blood glucose was measured from the tail vein using a glucometer, and insulin was measured in retro-orbital vein samples at the indicated time points.

Taste Preference

Taste preference during peptide treatment was evaluated between regular chow and a palatable medium-fat, high-sucrose diet (condensed milk diet, D12266B; Research Diets). Single-housed DIO mice were provided with both diets in separate compartments in the wire cage top equidistant from the water bottle. Fresh diet was provided daily. Baseline preference was assessed during 6 days. After this, mice were divided into treatment groups with comparable baseline diet preference and body weight, and diet preference was assessed in two separate experiments. First, mice had 2 days' access to either chow or condensed milk diet followed by 2 days' access to the same diet during treatment with vehicle, P-NT (396 nmol/kg), liraglutide (2 nmol/kg), or combination treatment. After a 1-week washout period, the mice were switched to the opposite diet and the protocol was repeated, and the ability of the treatments to inhibit the intake of the two diets was compared. Another cohort of DIO mice had access to both diets simultaneously during peptide injections, and the data are presented as intake of condensed milk diet/ total intake.

Electrophysiology

Pomc-hrGFP mice (21) were used to identify Pomc neurons in the arcuate nucleus of the hypothalamus. Brain slices were prepared from male mice (5–8 weeks old), and electrophysiology was performed as previously described (25–27). NT (100 nmol/L) (PolyPeptide Laboratories, Hillerød, Denmark), liraglutide (100 nmol/L), and tetrodotoxin (TTX) (2 μmol/L) (Tocris, Bristol, U.K.) were added to the artificial cerebrospinal fluid for specific experiments. Solutions containing drug were typically perfused for 5 min. A drug effect was required to be associated temporally with peptide application, and the response had to be stable within a few min. A neuron was considered depolarized if a change in membrane potential was at least 2 mV in amplitude. *n* represents the number of cells studied.

Multiplex Fluorescence In Situ Hybridization

Brains from lean wild-type mice were frozen in powdered dry ice and sectioned on a cryostat into 12-μm-thick coronal sections that were collected from the arcuate nucleus. In situ hybridization was performed according to manufacturers' instructions using the RNAscope Multiplex Fluorescent Reagent Kit v2 (Advanced Cell Diagnostics [ACD], Newark, CA) and PerkinElmer TSA Plus Fluorescein, Cyanine 3, and Cyanine 5 systems (PerkinElmer, Waltham, MA). Probes targeting mm-Pomc (cat. no. 314081-C3; ACD), mm-NtsR1 (cat. no. 422411; ACD), mm-GLP-1R (cat. no. 418851-C2; ACD), mm-Ppib (cat. no. 313911; ACD), and DapB (cat. no. 310043; ACD) were used. Images were captured using a laser scanning confocal microscope (LSM700; Zeiss).
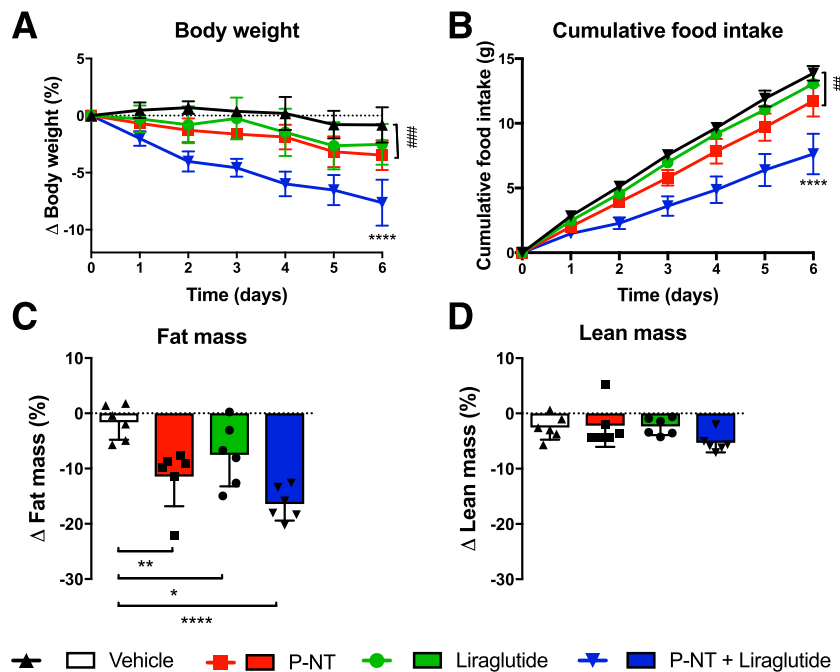
Figure 1—Metabolic effects of P-NT, liraglutide, and P-NT plus liraglutide combination therapy in obese mice during 6 days' treatment. Body weight (*A*), cumulative food intake (*B*), fat mass (*C*), and lean mass (*D*) following treatment with vehicle, P-NT (396 nmol/kg), liraglutide (8 nmol/kg), or combination treatment with P-NT (396 nmol/kg) and liraglutide (8 nmol/kg). *$P < 0.05$, **/##$P < 0.01$, ###$P < 0.001$ ****$P < 0.0001$. **** in *A* and *B* denotes difference between combination treatment and all other conditions. Data tested with two-way ANOVA repeated measurements with Tukey multiple comparison test for individual time points (*A* and *B*) and one-way ANOVA with Sidak multiple comparison test (*C* and *D*). Data are mean ± SD. $n = 6$.

Statistics

Data were tested for statistical significance using Graph-Pad Prism except for ANCOVA, which was performed using SAS. *t* test, Mann-Whitney nonparametric test, two-way ANOVA repeated measurements, two-way ANOVA, and one-way ANOVA were performed with appropriate multiple comparisons tests as indicated in figure legends. Energy expenditure data were analyzed using ANCOVA with body weight as the covariate. All data are represented as mean ± SD. The level of significance was set at $P < 0.05$.

RESULTS

Combination Treatment With P-NT and Liraglutide Reduces Body Weight and Food Intake in DIO Mice

Optimization of the P-NT dose showed that increasing the dose from 396 nmol/kg to 1,188 nmol/kg both as a mono-therapy and in combination with liraglutide did not result

in improved weight loss or food intake inhibition (Supplementary Fig. 1*A* and *B*). Decreasing the P-NT dose below 396 nmol/kg to 132 nmol/kg and 44 nmol/kg negatively impacted the ability of P-NT to reduce food intake and body weight as a monotherapy; however, in combination with liraglutide, the 132 nmol/kg dose showed efficiency equal to that of the 396 nmol/kg dose (Supplementary Fig. 1*C* and *D*). For remaining experiments, the 396 nmol/kg dose was used.

During 6 days of daily treatment, P-NT monotherapy reduced food intake and body weight, while liraglutide was not significantly different from vehicle-treated mice. Mice cotreated with P-NT and liraglutide lost ~8% (4 g) of their body weight, and a synergistic effect of the peptides was observed on feeding inhibition and body weight loss (Fig. 1*A* and *B*). The weight loss was predominantly due to loss of fat mass (Fig. 1*C* and *D*). Mice in the combination treatment group had decreased insulin and leptin levels

Table 1—Blood biochemistry

	Vehicle	Liraglutide (8 nmol/kg)	P-NT (396 nmol/kg)	P-NT (396 nmol/kg) plus liraglutide (8 nmol/kg)
Triglycerides (mg/dL)	95.1 ± 15.2	82.2 ± 9.0	100.4 ± 17.4	82.2 ± 15.7
Leptin (pg/mL)	48.1 ± 9.9	42.3 ± 11.8	35.4 ± 12.7	21.7 ± 3.5*
Insulin (ng/mL)	6.4 ± 3.0	5.3 ± 2.2	4.9 ± 2.4	2.3 ± 1.9*
Glucose (mmol/L)	8.3 ± 0.9	6.7 ± 0.9**	8.4 ± 0.8	6.4 ± 0.4**

Values denote mean ± SD. *$P < 0.05$ difference against vehicle. **$P < 0.01$ difference against vehicle and P-NT. Data tested with one-way ANOVA with Tukey multiple comparison test. $n = 6$.

compared with vehicle, reflecting the weight loss in this group (Table 1). Mice treated with P-NT and liraglutide combination treatment also had lower glucose levels, and this appeared to be driven by liraglutide (Table 1).

Combination Treatment With P-NT and Liraglutide Does Not Affect Energy Expenditure or Induce a Taste Aversion

For further understanding of the mechanism for the observed weight loss, indirect calorimetry was performed. No differences were observed between groups in energy expenditure and activity levels (Fig. 2A–C), while a reduction in the RER value was found after combination treatment reflecting increased lipid oxidation (Fig. 2D). Food intake and body weight were reduced in a synergistic manner following P-NT and liraglutide combination treatment relative to monotherapies (Fig. 2E and F). Vehicle-treated mice that were pair fed to the combination treatment had a weight loss similar to that of the combination treatment group, suggesting that energy expenditure did not contribute to the phenotype (Fig. 2G). For establishment of whether the decreased food intake could be due to nausea as previously described for peak doses of liraglutide (28–30), a taste aversion experiment was performed. P-NT, subthreshold liraglutide dose, or the combination of P-NT and liraglutide did not cause a conditioned taste aversion, whereas injections of the positive control LiCl induced an aversion toward saccharin (Fig. 2H).
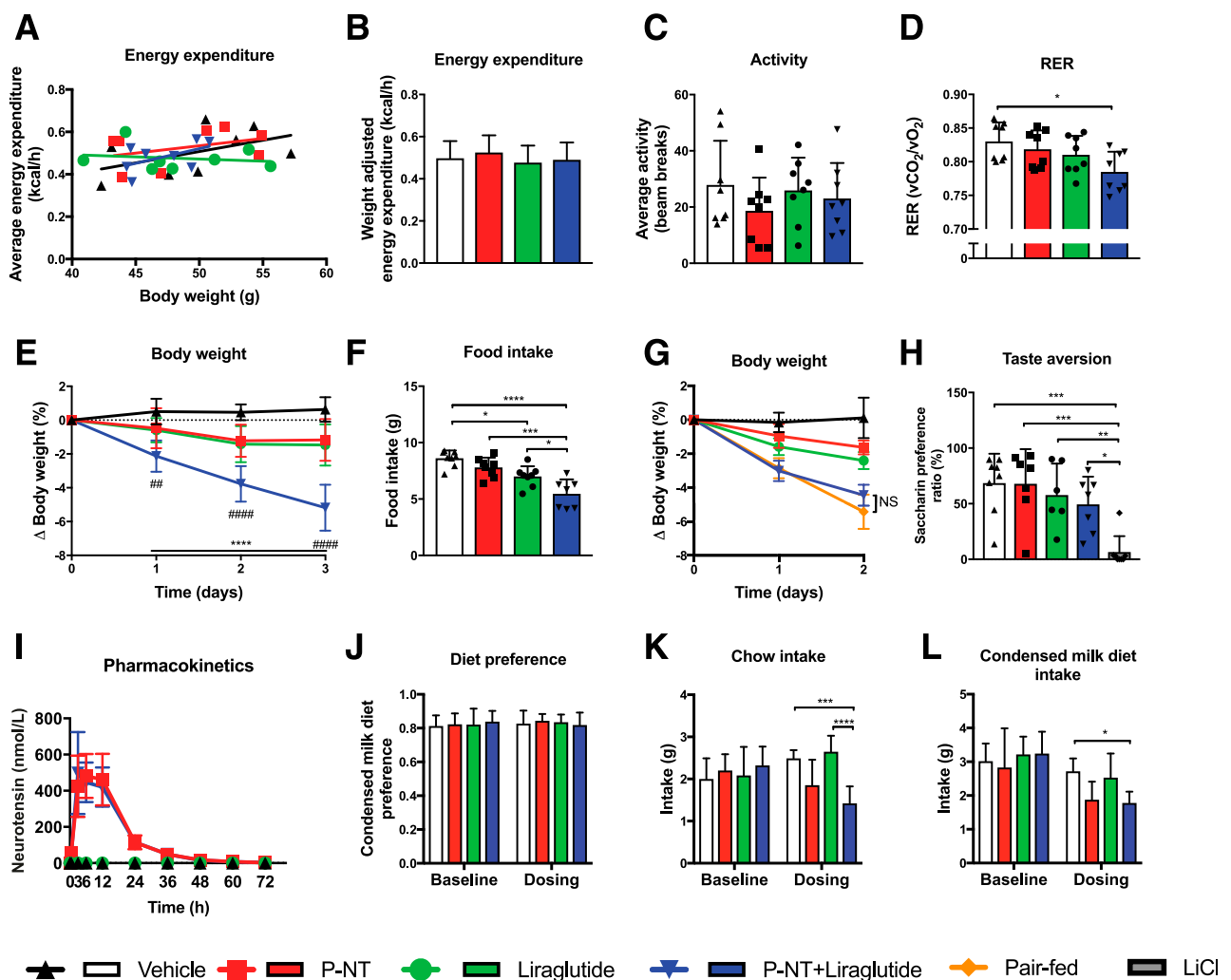
Figure 2—Indirect calorimetry, taste aversion, pharmacokinetics, and taste preference. Energy expenditure (A), weight-adjusted energy expenditure (B), activity levels (C), RER (D), body weight (E), food intake (F), body weight with pair feeding (G), saccharin preference ratio during taste aversion (H), intact NT levels following peptide injections (I), taste preference with simultaneous two-diet access (J), and food intake inhibition on a chow versus a palatable medium-fat, high-sucrose diet (condensed milk diet) (K and L). *$P < 0.05$; **/##$P < 0.01$; ***$P < 0.001$; ****/####$P < 0.0001$. **** in E denotes difference between combination treatment and vehicle, while ##/#### denote differences between P-NT and liraglutide monotreatment and combination treatment. Data tested with ANCOVA (A and B), one-way ANOVA with Sidak multiple comparison test (C, D, F, and H), two-way ANOVA repeated measurements with Tukey multiple comparison test for individual time points (E), and two-way ANOVA with Tukey multiple comparison test (J–L). Data are mean ± SD. $n = 8$ (A–F, H, and J–L), $n = 5$ (G), and $n = 4$ (I). Liraglutide dosed in a concentration of 2 nmol/kg (A–F and J–L) and 3 nmol/kg (G–I).
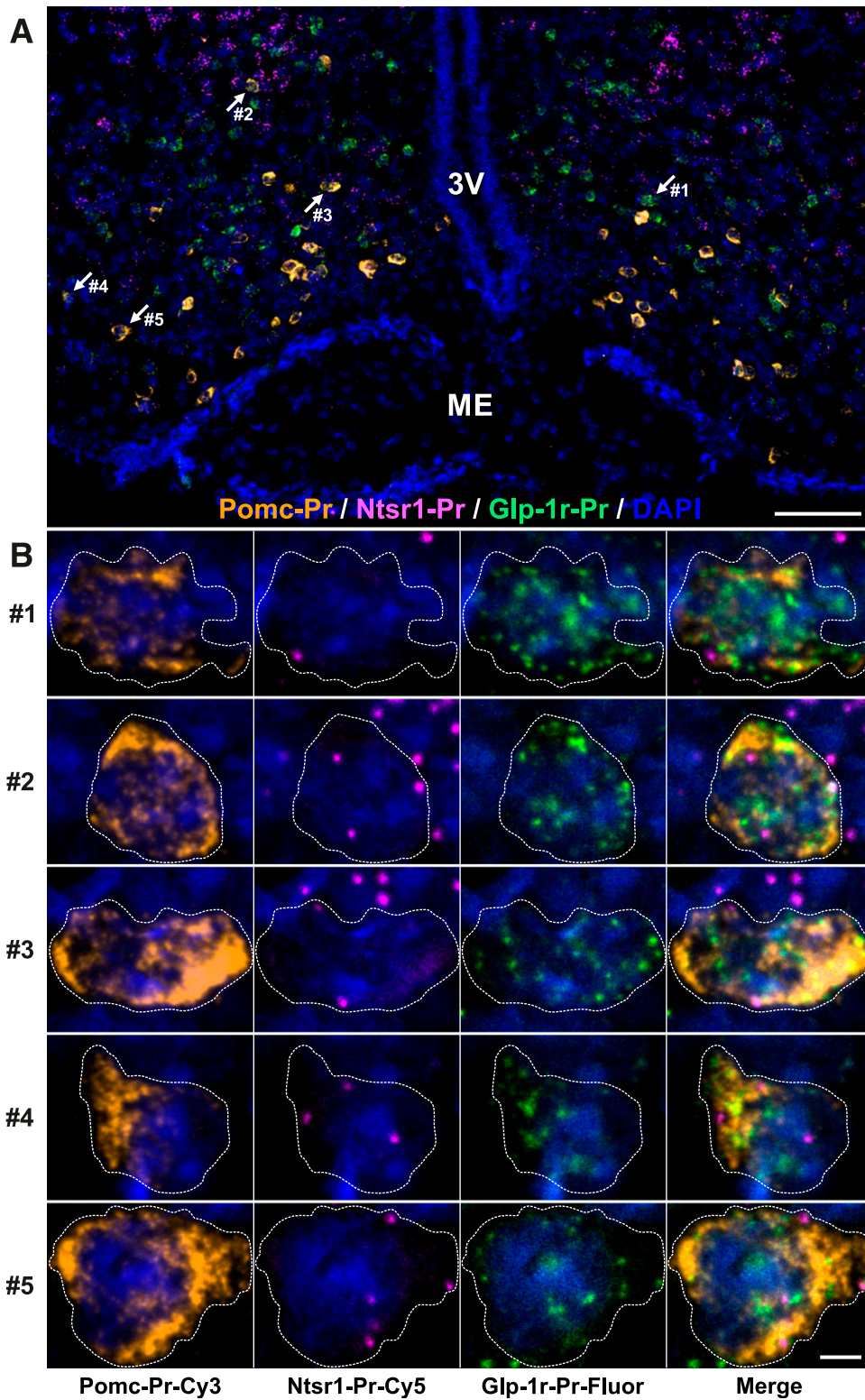
Figure 3—Multiplex fluorescence in situ hybridization (M-FISH) staining of GLP-1R, NtsR1, and Pomc mRNA in the murine arcuate nucleus. *A*: Representative merged confocal image of arcuate nucleus section costained with probes (Pr) specific for GLP-1R (green), NtsR1 (magenta), and Pomc (orange) mRNA transcripts using M-FISH and counterstained with DAPI (blue). Arrows show cells in higher magnification in *B*. Scale bar = 100 μm. *B*: Selected areas from above showing neurons costained with Pomc (orange [column 1]), NtsR1 (magenta [column 2]), and GLP-1R (green [column 3]) transcripts and a merged picture (column 4). Dashed lines outline cytosol border. Scale bar = 5 μm. ME, median eminence; 3V, 3rd ventricle.
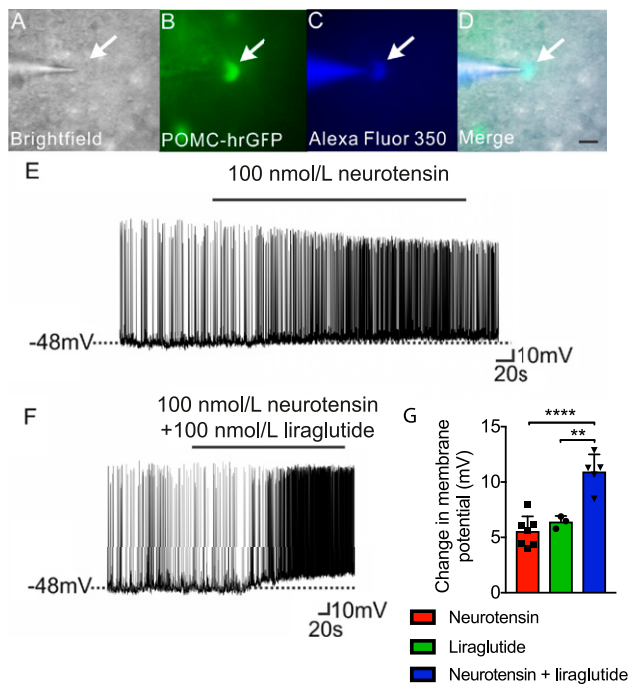
Figure 4—NT and liraglutide effects on Pomc neuron activity. Bright-field illumination of Pomc-hrGFP neuron (*A*), the neuron under FITC (hrGFP) illumination (*B*), and complete dialysis of Alexa Fluor 350 from the intracellular pipette (*C*). *D*: Merged image illustrates colocalization of brightfield, hrGFP, and Alexa Fluor 350 indicative of a Pomc neuron. Scale bar = 50 μm. *E*: Current-clamp recording demonstrates that NT (100 nmol/L) depolarized Pomc neurons. *F*: Current-clamp recording demonstrates a Pomc-hrGFP neuron is depolarized by NT (100 nmol/L) and liraglutide (100 nmol/L). *G*: NT, liraglutide, and combination treatment induced change in membrane potential. Data are mean ± SD. **$P < 0.01$; ****$P < 0.0001$. Data tested with one-way ANOVA with Tukey multiple comparison test (n = 3–7).

The exposure time in plasma of P-NT was similar when administered alone or in combination with liraglutide, and plasma NT levels were elevated above baseline for up to 48 h (Fig. 2*I*). In comparison, native NT is cleared in just 15 min using the same method (16). Finally, we assessed whether P-NT and liraglutide mono- and combination treatment affected taste preference. When mice were given the choice between chow and a palatable medium-fat, high-sucrose diet (condensed milk diet), we found no changes in their diet preference following peptide treatment (Fig. 2*J*). Further, we found no differences in the ability of P-NT and liraglutide mono- and combination treatment to inhibit the intake of chow versus the condensed milk diet, indicating that the treatments did not affect taste preference (Fig. 2*K* and *L*).

The Melanocortin System Is Central for P-NT and P-NT and Liraglutide Combination Treatment Efficacy
In accordance with previous publications (31,32), we found that NtsR1 and GLP-1R were expressed in Pomc neurons in the arcuate nucleus and that numerous Pomc neurons coexpressed both NtsR1 and GLP-1R using in situ hybridization (Fig. 3*A* and *B* [positive and negative controls]) (Supplementary Fig. 2). Next, we assessed whether NT

increases the firing rate of arcuate Pomc neurons in Pomc-eGFP mice. NT (100 nmol/L) depolarized Pomc neurons (change of resting membrane potential: increase of 5.5 ± 0.5 mV [n = 7]) (Fig. 4*A*–*E* and *G*). Similar to previous reports studying GLP-1 (31), we found that liraglutide (100 nmol/L) depolarized Pomc neurons to a similar degree (change of resting membrane potential: increase of 6.4 ± 0.3 mV [n = 3]) (Fig. 4*G*). Notably, combined administration with NT (100 nmol/L) and liraglutide (100 nmol/L) resulted in a larger depolarization of Pomc neurons (change of resting membrane potential: increase of 10.9 ± 0.7 mV [n = 5]) (Fig. 4*F* and *G*). These data suggest that liraglutide can enhance the NT-induced excitatory effect on Pomc neurons. The depolarization induced by NT and combination treatment with NT and liraglutide was observed in the presence of TTX (2 μmol/L [increase of 7.4 ± 0.2 mV] [NT], n = 4, and 11.5 ± 2.0 mV [NT plus liraglutide], n = 5) (Supplementary Fig. 3*A*–*C*), indicative of a direct membrane depolarization independent of action potential–mediated synaptic transmission.

Finally, we tested the effect of P-NT and liraglutide mono- and combination therapy in MC4R KO mice compared with weight-matched DIO controls during 3 days of treatment. MC4R KO mice were unresponsive to the anorexigenic and body weight–reducing effect of P-NT (Fig. 5*B* and *E*). MC4R KO and DIO control mice showed no response to subthreshold liraglutide monotherapy (Fig. 5*A* and *D*); however, a 10× dose of liraglutide evoked a larger anorexic and body weight–reducing response in DIO control mice compared with MC4R KO mice (Supplementary Fig. 4*A* and *B*). MC4R KO mice decreased their food intake and body weight after P-NT and liraglutide combination therapy, but their response was blunted compared with DIO controls (Fig. 5*C* and *F*). Loss of fat and lean mass was, likewise, blunted in MC4R KO mice compared with DIO controls following P-NT monotherapy and P-NT and liraglutide combination therapy (Fig. 5*G* and *H*), overall suggesting that the melanocortin pathway is important for P-NT–induced appetite regulation and body weight reduction.

Acute P-NT and Liraglutide Combination Treatment Does Not Affect Glucose Tolerance
We evaluated the acute effect of P-NT and liraglutide treatment on glucose homeostasis using an oral glucose tolerance test in DIO mice. P-NT lowered the glucose level at the 15-min time point compared with vehicle and liraglutide monotherapy (Fig. 6*A*). However, overall, no differences in glucose levels (area under the curve) were observed between groups (Fig. 6*B*), as P-NT slightly delayed the glucose excursion. Insulin levels were likewise similar after acute peptide treatment (Fig. 6*C*).

P-NT and Liraglutide Combination Treatment Reduces Steatohepatitis
We observed a modest improvement in steatohepatitis in the P-NT and the P-NT and liraglutide combination treatment group in DIO mice after 6 days of treatment (Fig. 7*A*
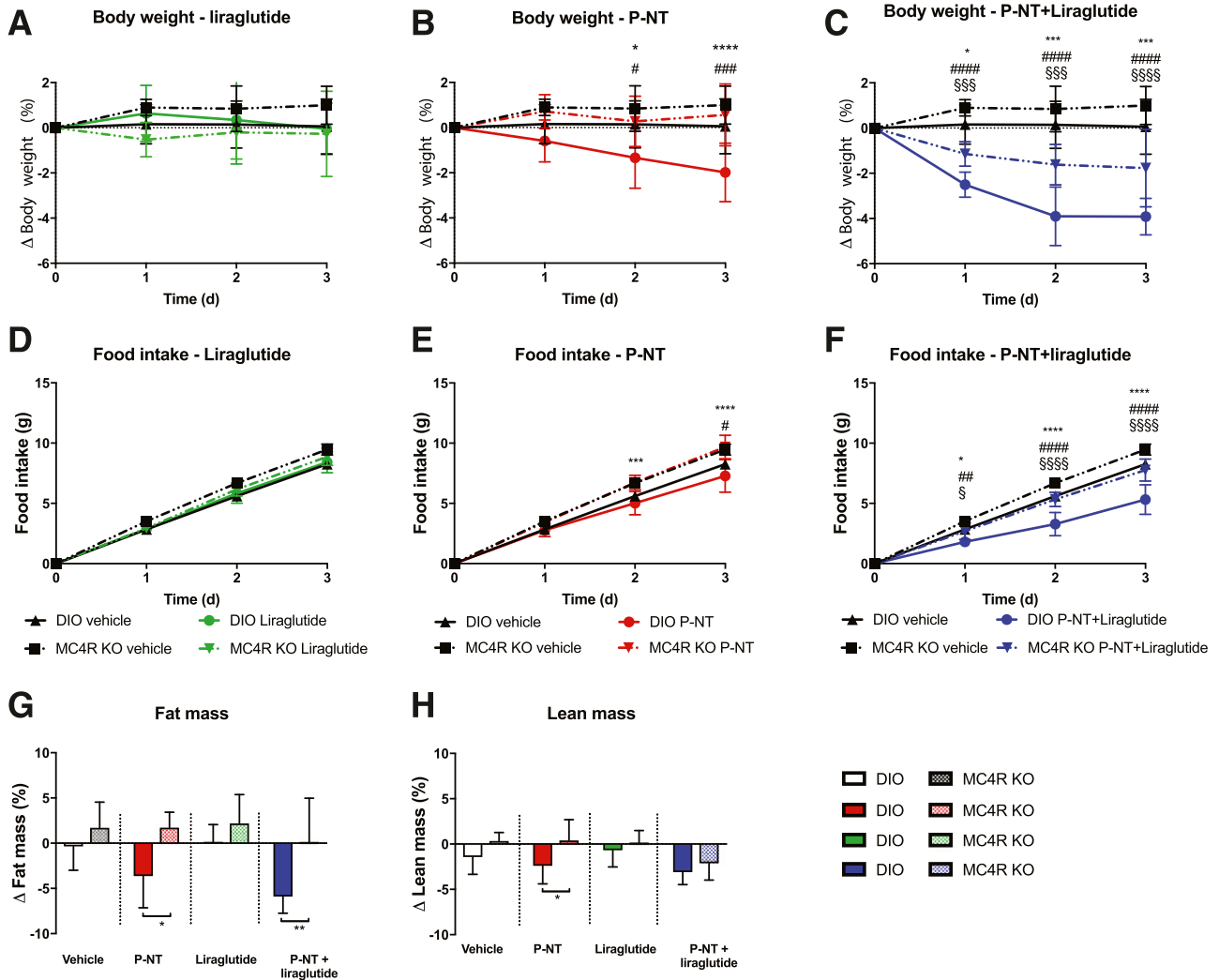
Figure 5—Role of the melanocortin system for P-NT, liraglutide, and combination therapy effects. *A*: Body weight loss following liraglutide (2 nmol/kg) treatment. *B*: Body weight loss following P-NT (396 nmol/kg) treatment. *C*: Body weight loss following P-NT (396 nmol/kg) plus liraglutide (2 nmol/kg) treatment. *D*: Cumulative food intake following liraglutide (2 nmol/kg) treatment. *E*: Cumulative food intake following P-NT (396 nmol/kg) treatment. *F*: Cumulative food intake following P-NT (396 nmol/kg) plus liraglutide (2 nmol/kg) treatment. *G*: Change in fat mass. *H*: Change in lean mass. Data represent differences between MC4R KO mice and weight-matched DIO controls during 3 days' treatment. */#/§$P < 0.05$; **/##$P < 0.01$; ***/###/§§§$P < 0.001$; ****/####/§§§§$P < 0.0001$. */**/***/**** represent differences between DIO treatment and MC4R KO treatment, #/##/###/#### represent differences between DIO vehicle and DIO treatment, and §/§§§/§§§§ represent differences between MC4R KO vehicle and MC4R KO treatment. Data tested with two-way ANOVA repeated measurements with Tukey multiple comparison test for individual time points (*A*–*F*) and two-way ANOVA with Sidak multiple comparison test (*G* and *H*). Data are mean ± SD. *n* = 6. d, days.

and *B*). This was accompanied by a reduction in *PCSK9* expression in the combination treatment group suggestive of increased removal of cholesterol from circulation, while major hepatic bile acid metabolism pathways were not regulated (Fig. 7*C* and *D*). Although total plasma cholesterol was not statistically different between groups (Fig. 7*E*), LDL cholesterol was substantially reduced in the combination treatment group, while HDL cholesterol showed a more modest decrease (Fig. 7*F*).

DISCUSSION

The lack of safe and effective pharmacotherapies to treat obesity and associated disorders, combined with a growing burden of metabolic diseases worldwide, highlights the

need for new treatment strategies. A pioneering approach to improve pharmacological efficacy has focused on combination therapies to obtain superior efficacy and better tolerability compared with monotherapies. In the current study, we find that a pegylated version of the gut hormone NT reduced food intake, body weight, and adiposity in DIO mice. Intriguingly, when P-NT was combined with a subthreshold dose of the GLP-1 mimetic liraglutide, the two peptides exerted a synergistic reduction in body weight and food intake in obese mice relative to each monotherapy. Our indirect calorimetry and pair-feeding data suggest that altered activity and energy expenditure were not contributing to the weight phenotype. Further, glucose homeostasis and liver function were improved
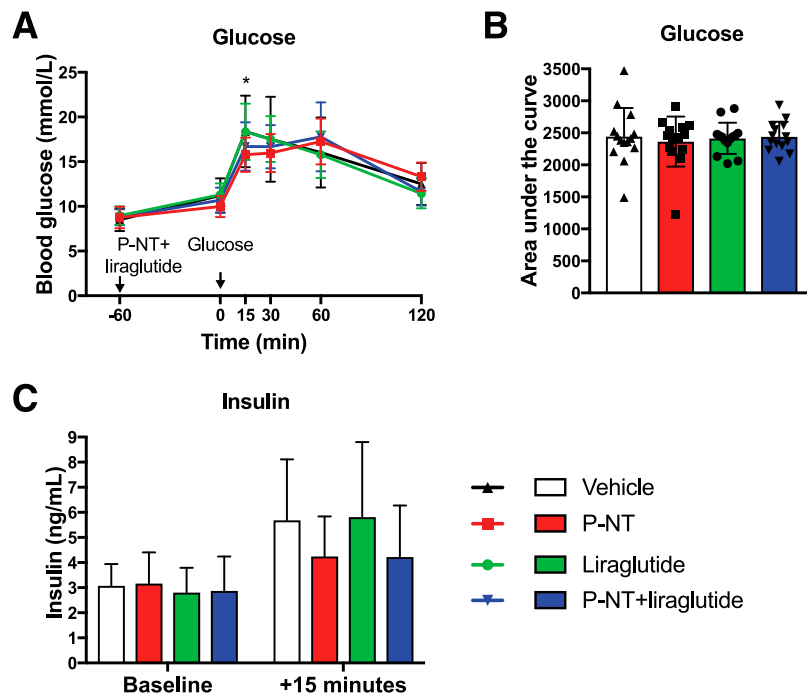
Figure 6—Glucose tolerance after acute treatment with P-NT, liraglutide, and P-NT plus liraglutide combination therapy in DIO mice. *A*: Glucose levels at individual time points. *B*: Glucose area under the curve. *C*: Insulin levels at individual time points following vehicle, P-NT (396 nmol/kg), liraglutide (2 nmol/kg), or combination treatment with P-NT (396 nmol/kg) and liraglutide (2 nmol/kg). *Difference between P-NT and liraglutide and P-NT and vehicle. Data tested with two-way ANOVA repeated measurements with Tukey multiple comparison test (*A*), one-way ANOVA with Tukey multiple comparison test (*B*), and two-way ANOVA with Tukey multiple comparison test (*C*). Data are mean ± SD. *n* = 14.

following chronic liraglutide and combination treatment, respectively, demonstrating an overall improvement in metabolic disorders. Finally, we found that the melanocortin pathway is central for the anorexigenic effect of P-NT and the synergy observed between liraglutide and P-NT.

Currently, liraglutide monotherapy constitutes one of the safest treatment options for obesity but only elicits modest weight loss in humans (2), and problems with compliance exist mainly due to nausea, which is experienced by upwards of 30–40% of patients (4,5). This is likewise seen in rodents where peak doses of liraglutide induce a taste aversion toward associated flavors (28–30). Thus, it is desirable to improve tolerability by using lower liraglutide doses while maintaining efficacy by combining it with another weight-reducing agent that does not evoke nausea and emesis. In the current study, we demonstrate this principle by combining liraglutide with P-NT. Subthreshold dosing of the monotherapies give rise to modest improvements in body weight, but when administered in combination, liraglutide and P-NT synergize to amplify anorexigenic signaling without inducing taste aversion. NT has previously been described to have varying effects on glucose homeostasis (33). Here, we found that acute treatment with P-NT and subthreshold liraglutide mono- and combination therapy did not result in improvements in glucose control or insulin levels. However, following 6 days' treatment, glucose and insulin levels significantly improved in mice that were treated with liraglutide and the combination of P-NT and liraglutide, suggesting that liraglutide drives the chronic benefits on glucose metabolism.

We also observed modest improvements in steatohepatitis, decreased plasma LDL cholesterol, and changes in liver gene expression suggestive of improved hepatic lipid handling and removal of cholesterol from the blood following 6 days of combination treatment in DIO mice. Recent clinical studies report discrepant results regarding the association between circulating pro-NT or NT levels and nonalcoholic fatty liver disease (34,35). Although previous studies report the presence of NtsR1 in the liver in some species (36,37), we did not find any NtsR1 expression in mouse liver using quantitative PCR (data not shown). The lack of NtsR1 expression in liver is supported by results in human and mouse databases (www.proteinatlas.org, www.informatics.jax.org/assay/MGI:3625053). Therefore, the reduced steatohepatitis in our study is most likely an indirect mechanism potentially contributable to the weight loss of the mice.

The downstream mechanism by which peripheral NT reduces food intake is largely unexplored. We previously showed that NT-induced anorexia persists in vagotomized mice, pointing to a direct effect in the brain of NT (16).
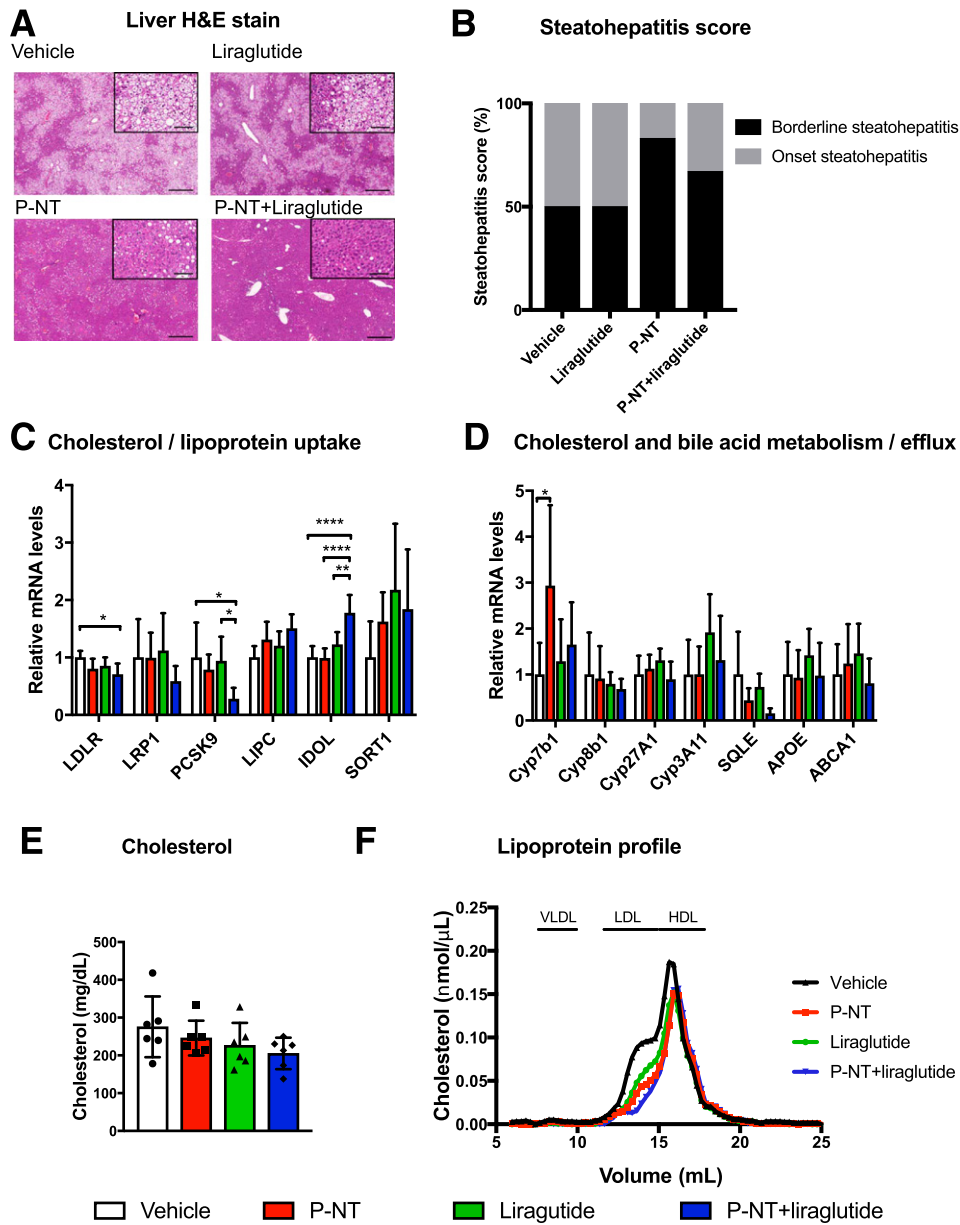
Figure 7—Effects of 6 days' treatment with P-NT, liraglutide, or combination therapy on liver function and plasma cholesterol. H-E stain (scale bar = 500 μm/zoom = 100 μm) (*A*), steatohepatitis score (*B*), hepatic gene expression related to cholesterol/lipoprotein uptake (*C*), hepatic gene expression related to cholesterol and bile acid metabolism/efflux (*D*), total cholesterol (*E*), and lipoprotein profile (*F*) following vehicle, P-NT (396 nmol/kg), liraglutide (8 nmol/kg), and P-NT (396 nmol/kg) plus liraglutide (8 nmol/kg) treatment. *$P < 0.05$; **$P < 0.01$; ****$P < 0.0001$. Data tested with Student t test (*C* and *D*) and one-way ANOVA with Tukey multiple comparison test (*E*). Data are mean ± SD. $n = 6$.

NtsR1 is widely expressed centrally with high levels in both homeostatic, i.e., hypothalamus, and hedonic, i.e., the ventral tegmental area, food intake–regulating regions (38). Due to the size and hydrophilic nature of the PEG modification of our NT peptide, the effects seen in the current study are more likely to be mediated via brain areas with a compromised blood-brain barrier such as the arcuate nucleus of the hypothalamus. This is supported by our taste preference data, showing that P-NT and liraglutide mono- and combination treatment exert the same level of inhibition on diets of varying palatability, pointing to homeostatic feeding regulation. In the arcuate nucleus, NtsR1 is present on both Pomc and AgRP neurons (32). Following acute P-NT treatment, we previously observed an upregulation of Pomc expression in the arcuate nucleus, while AgRP and NPY were not regulated (16). Thus, here we focused on Pomc neurons in our characterization of the downstream effectors of P-NT and liraglutide therapy. We found that Pomc neurons coexpressed NtsR1 and GLP-1R. Further, Pomc neurons were depolarized in response to NT, and the change in membrane potential was augmented with liraglutide coapplication. These effects persisted in

the presence of TTX, indicative of a direct effect on Pomc neurons independent of synaptic transmission. Next, we assessed the effect of P-NT and liraglutide mono- and combination therapy in MC4R KO mice in comparison with weight-matched DIO control mice. MC4R KO mice were unresponsive to the anorexic and body weight–lowering effects of P-NT monotherapy and showed a blunted response to P-NT and liraglutide combination therapy. This suggests that the melanocortin pathway is essential for P-NT–induced anorexia and necessary for P-NT and liraglutide to synergize in their regulation of food intake and body weight. Liraglutide reduces food intake when microinjected into the arcuate nucleus (39), and Pomc neurons have been suggested as important downstream effectors of liraglutide-induced anorexia (31). However, others have challenged the necessity of Pomc neurons for liraglutide to reduce food intake (30,40,41), and a model where several sites and neuronal populations in the brain contribute to liraglutide-induced anorexia is emerging (42). As the anorexigenic and body weight–lowering effects of medium-dose liraglutide monotherapy (20 nmol/kg) were blunted in MC4R KO mice compared with DIO controls in our study, our data suggest that liraglutide can partly act through this pathway. We therefore hypothesize that NT and liraglutide converge on the same population of Pomc neurons to reverse obesity but through different intracellular signaling pathways, as NT is $G\alpha_q$-coupled, while GLP-1 acts through $G\alpha_s$. The $G\alpha_q$ and $G\alpha_s$ signaling pathways have previously been described to synergize in other cellular systems (43). Future studies should map out the exact contribution of the different intracellular signaling events underlying the observed synergy between P-NT and liraglutide.

In conclusion, we developed a stable long-acting analog of NT, enabling us to establish the impact of sustained NT signaling on metabolic homeostasis. We demonstrate a synergistic action between GLP-1 and NT-mediated pathways in the regulation of food intake and body weight and show that P-NT in combination with subthreshold doses of liraglutide reverses obesity and metabolic syndrome without the concurrent induction of nausea seen with peak dose liraglutide monotherapy. Finally, we identify the melanocortin pathway as a key downstream effector circuit for P-NT action in the brain and suggest that P-NT and liraglutide may synergize in Pomc neurons via segregated intracellular signaling pathways.

Author Contributions. C.R. co-conceptualized, researched, and interpreted data and wrote the manuscript. Z.H. and K.W.W. performed electrophysiology studies and interpreted data. K.V.G., L.J.S., B.Ha., A.B., and C.Ch. researched and interpreted data and reviewed the manuscript. F.Z. and M.H.T. provided resources. A.F. performed liver histology. B.F., R.D.D., and G.M.L. provided resources and reviewed the manuscript. C.Cl. co-conceptualized, researched, and interpreted data and reviewed the manuscript. B.Ho. co-conceptualized and interpreted data and reviewed the manuscript. C.R., Z.H., K.V.G., L.J.S., B.Ha., F.Z., A.F., A.B., C.Ch., M.H.T., B.F., R.D.D., G.M.L., K.W.W., C.Cl., and B.Ho. approved the manuscript. C.R. is the guarantor of this work and, as such, had full access to all the data in the study and takes responsibility for the integrity of the data and the accuracy of the data analysis.

References

1. Wang YC, McPherson K, Marsh T, Gortmaker SL, Brown M. Health and economic burden of the projected obesity trends in the USA and the UK. Lancet 2011;378:815–825
2. Heymsfield SB, Wadden TA. Mechanisms, pathophysiology, and management of obesity. N Engl J Med 2017;376:254–266
3. Stefanidis A, Oldfield BJ. Neuroendocrine mechanisms underlying bariatric surgery: insights from human studies and animal models. J Neuroendocrinol 2017;29:e12534
4. Marino AB, Cole SW, Nuzum DS. Alternative dosing strategies for liraglutide in patients with type 2 diabetes mellitus. Am J Health Syst Pharm 2014;71:223–226
5. Bettge K, Kahle M, Abd El Aziz MS, Meier JJ, Nauck MA. Occurrence of nausea, vomiting and diarrhoea reported as adverse events in clinical trials studying glucagon-like peptide-1 receptor agonists: a systematic analysis of published clinical trials. Diabetes Obes Metab 2017;19:336–347
6. Finan B, Clemmensen C, Müller TD. Emerging opportunities for the treatment of metabolic diseases: glucagon-like peptide-1 based multi-agonists. Mol Cell Endocrinol 2015;418:42–54
7. Müller TD, Sullivan LM, Habegger K, et al. Restoration of leptin responsiveness in diet-induced obese mice using an optimized leptin analog in combination with exendin-4 or FGF21. J Pept Sci 2012;18:383–393
8. Neary NM, Small CJ, Druce MR, et al. Peptide YY3-36 and glucagon-like peptide-17-36 inhibit food intake additively. Endocrinology 2005;146:5120–5127
9. Trevaskis JL, Sun C, Athanacio J, et al. Synergistic metabolic benefits of an exenatide analogue and cholecystokinin in diet-induced obese and leptin-deficient rodents. Diabetes Obes Metab 2015;17:61–73
10. Trevaskis JL, Mack CM, Sun C, et al. Improved glucose control and reduced body weight in rodents with dual mechanism of action peptide hybrids. PLoS One 2013;8:e78154
11. Finan B, Yang B, Ottaway N, et al. A rationally designed monomeric peptide triagonist corrects obesity and diabetes in rodents. Nat Med 2015;21:27–36
12. Grunddal KV, Ratner CF, Svendsen B, et al. Neurotensin is coexpressed, coreleased, and acts together with GLP-1 and PYY in enteroendocrine control of metabolism. Endocrinology 2016;157:176–194
13. Cooke JH, Patterson M, Patel SR, et al. Peripheral and central administration of xenin and neurotensin suppress food intake in rodents. Obesity (Silver Spring) 2009;17:1135–1143
14. de Beaurepaire R, Suaudeau C. Anorectic effect of calcitonin, neurotensin and bombesin infused in the area of the rostral part of the nucleus of the tractus solitarius in the rat. Peptides 1988;9:729–733

15. Hawkins MF, Barkemeyer CA, Tulley RT. Synergistic effects of dopamine agonists and centrally administered neurotensin on feeding. Pharmacol Biochem Behav 1986;24:1195–1201

16. Ratner C, Skov LJ, Raida Z, et al. Effects of peripheral neurotensin on appetite regulation and its role in gastric bypass surgery. Endocrinology 2016;157:3482–3492

17. Dirksen C, Jørgensen NB, Bojsen-Møller KN, et al. Gut hormones, early dumping and resting energy expenditure in patients with good and poor weight loss response after Roux-en-Y gastric bypass. Int J Obes 2013;37:1452–1459

18. Näslund E, Grybäck P, Hellström PM, et al. Gastrointestinal hormones and gastric emptying 20 years after jejunoileal bypass for massive obesity. Int J Obes Relat Metab Disord 1997;21:387–392

19. Aronin N, Carraway RE, Ferris CF, Hammer RA, Leeman SE. The stability and metabolism of intravenously administered neurotensin in the rat. Peptides 1982;3:637–642

20. Balthasar N, Dalgaard LT, Lee CE, et al. Divergence of melanocortin pathways in the control of food intake and energy expenditure. Cell 2005;123:493–505

21. Parton LE, Ye CP, Coppari R, et al. Glucose sensing by POMC neurons regulates glucose homeostasis and is impaired in obesity. Nature 2007;449:228–232

22. Christoffersen C, Jauhiainen M, Moser M, et al. Effect of apolipoprotein M on high density lipoprotein metabolism and atherosclerosis in low density lipoprotein receptor knock-out mice. J Biol Chem 2008;283:1839–1847

23. Jall S, Sachs S, Clemmensen C, et al. Monomeric GLP-1/GIP/glucagon triagonism corrects obesity, hepatosteatosis, and dyslipidemia in female mice. Mol Metab 2017;6:440–446

24. Kuhre RE, Bechmann LE, Wewer Albrechtsen NJ, Hartmann B, Holst JJ. Glucose stimulates neurotensin secretion from the rat small intestine by mechanisms involving SGLT1 and GLUT2, leading to cell depolarization and calcium influx. Am J Physiol Endocrinol Metab 2015;308:E1123–E1130

25. Sun J, Gao Y, Yao T, et al. Adiponectin potentiates the acute effects of leptin in arcuate Pomc neurons. Mol Metab 2016;5:882–891

26. Yao T, Deng Z, Gao Y, et al. Ire1α in Pomc neurons is required for thermogenesis and glycemia. Diabetes 2017;66:663–673

27. Gao Y, Yao T, Deng Z, et al. TrpC5 mediates acute leptin and serotonin effects via Pomc neurons. Cell Reports 2017;18:583–592

28. Sisley S, Gutierrez-Aguilar R, Scott M, D'Alessio DA, Sandoval DA, Seeley RJ. Neuronal GLP1R mediates liraglutide's anorectic but not glucose-lowering effect. J Clin Invest 2014;124:2456–2463

29. Kanoski SE, Rupprecht LE, Fortin SM, De Jonghe BC, Hayes MR. The role of nausea in food intake and body weight suppression by peripheral GLP-1 receptor agonists, exendin-4 and liraglutide. Neuropharmacology 2012;62:1916–1927

30. Adams JM, Pei H, Sandoval DA, et al. Liraglutide modulates appetite and body weight through glucagon-like peptide 1 receptor-expressing glutamatergic neurons. Diabetes 2018;67:1538–1548

31. Secher A, Jelsing J, Baquero AF, et al. The arcuate nucleus mediates GLP-1 receptor agonist liraglutide-dependent weight loss. J Clin Invest 2014;124:4473–4488

32. Henry FE, Sugino K, Tozer A, Branco T, Sternson SM. Cell type-specific transcriptomics of hypothalamic energy-sensing neuron responses to weight-loss. eLife 2015;4

33. Mazella J, Béraud-Dufour S, Devader C, Massa F, Coppola T. Neurotensin and its receptors in the control of glucose homeostasis. Front Endocrinol (Lausanne) 2012;3:143

34. Auguet T, Aragonès G, Berlanga A, et al. Low circulating levels of neurotensin in women with nonalcoholic fatty liver disease associated with severe obesity. Obesity (Silver Spring) 2018;26:274–278

35. Barchetta I, Cimini FA, Leonetti F, et al. Increased plasma proneurotensin levels identify NAFLD in adults with and without type 2 diabetes. J Clin Endocrinol Metab 2018;103:2253–2260

36. Méndez M, Souazé F, Nagano M, Kelly PA, Rostène W, Forgez P. High affinity neurotensin receptor mRNA distribution in rat brain and peripheral tissues. Analysis by quantitative RT-PCR. J Mol Neurosci 1997;9:93–102

37. Piątek J, Maćkowiak P, Krauss H, Nowak D, Bogdański P. In vivo investigations of neurotensin receptors in adipocytes, hepatocytes and enterocytes of rat. Ann Agric Environ Med 2011;18:433–436

38. Schroeder LE, Leinninger GM. Role of central neurotensin in regulating feeding: implications for the development and treatment of body weight disorders. Biochim Biophys Acta Mol Basis Dis 2018;1864:900–916

39. Beiroa D, Imbernon M, Gallego R, et al. GLP-1 agonism stimulates brown adipose tissue thermogenesis and browning through hypothalamic AMPK. Diabetes 2014;63:3346–3358

40. Nonogaki K, Kaji T. The acute anorexic effect of liraglutide, a GLP-1 receptor agonist, does not require functional leptin receptor, serotonin, and hypothalamic POMC and CART activities in mice. Diabetes Res Clin Pract 2016;120:186–189

41. Burmeister MA, Ayala JE, Smouse H, et al. The hypothalamic glucagon-like peptide 1 receptor is sufficient but not necessary for the regulation of energy balance and glucose homeostasis in mice. Diabetes 2017;66:372–384

42. Kanoski SE, Hayes MR, Skibicka KP. GLP-1 and weight loss: unraveling the diverse neural circuitry. Am J Physiol Regul Integr Comp Physiol 2016;310:R885–R895

43. Hauge M, Vestmar MA, Husted AS, et al. GPR40 (FFAR1) - combined Gs and Gq signaling in vitro is associated with robust incretin secretagogue action ex vivo and in vivo. Mol Metab 2014;4:3–14